

1
2 **Improved EPANET Hydraulic Model with Optimized Roughness Coefficient using**
3 **Genetic Algorithm**
4

5 **Chia-Cheng Shiu¹, Chih-Chung Chung^{2,*}, and Tzuping Chiang³**

6 ¹Department of Civil Engineering, National Central University; 110382004@cc.ncu.edu.tw

7 ²Department of Civil Engineering/Research Center for Hazard Mitigation and Prevention,
8 National Central University; ccchung@ncu.edu.tw

9 ³Department of Civil Engineering and Engineering Management, National Quemoy University;
10 ziping@nqu.edu.tw

11
12
13 Chih-Chung Chung, Associate Professor (ccchung@ncu.edu.tw)

14 Dept. of Civil Engineering/Research Center for Hazard Mitigation and Prevention, National
15 Central University, 300 Zhongda, Rd., Zhongli Dist., Taoyuan, 320, Taiwan.

16 Phone: +886-3-422-7151 ext. 34120

17 Fax: +886-3-425-2960

18
19
20 **Key Points:**

- 21 • The study proposed the integration of GA Algorithm with EPANET hydraulic model.
22 • The roughness can be optimized by considering pipe's material and spatial distributions.
23 • Simulation with the optimized roughness was highly correlated (0.9) with the field data.
24
25
26
27
28
29
30
31
32

33 Abstract

34 The process of calibrating hydraulic models for water distribution systems (WDS) is
35 crucial during the model-building process, particularly when determining the roughness
36 coefficients of pipes. However, using a single roughness coefficient based solely on pipe
37 material can lead to significant variations in frictional head losses. To address this issue and
38 enhance computational efficiency, this study proposes a single-objective procedure that utilizes
39 Genetic Algorithm (GA) for optimizing roughness coefficients in the EPANET hydraulic model.
40 EPANET-GA incorporates an automated calibration process and a User Graphic Interface (GUI)
41 to analyze the water head pressures of WDS nodes. Notably, the proposed method not only
42 optimizes roughness coefficients based on pipe material but also spatial characteristics of pipes.
43 To demonstrate the effectiveness of this method, the study builds a hydraulic analysis model for
44 the Zhonghe and Yonghe district of the Taipei Water Department, integrating graph theory's
45 connectivity and the GIS database. The model was optimized with 34,783 node items, 30,940
46 pipes, and 140 field measurements. Results show that the optimized roughness coefficient
47 produces a high correlation coefficient (0.9) with the measured data in a certain time slot.
48 Furthermore, a low standard error (8.93%) was achieved compared to 24-hour monitoring data.
49 The proposed method was further compared to WaterGEMs, and the study concludes that the
50 proposed model provides a reliable reference for the design and routing scenario of WDS.

51

52 Keyword: water distribution systems (WDS); Genetic Algorithm (GA); EPANET hydraulic
53 model; roughness coefficient

54

55 1 Introduction

56 In the present day, hydraulic simulation models have become widely utilized for
57 analyzing the behavior of water distribution systems (WDS), as noted by [Zanfei et al. \(2020\)](#) and
58 [Sitzenfrei et al. \(2020\)](#). The calibration of water distribution models involves adjusting network
59 parameters, such as pipe roughness and nodal demand ([Savic et al., 2009](#)), to minimize the
60 disparities between simulated results and real measurements. Over the last thirty years,
61 calibration has been a popular research topic among WDS analysts, and there have been
62 numerous publications on this subject in scientific and engineering literature. In their work,
63 [Savic et al. \(2009\)](#) conducted a comprehensive review of the calibration of water distribution
64 network models and classified the calibration methods into three categories.

65 The first category involves iterative procedure models, where unknown parameters are
66 updated at each iteration by solving the set of steady-state mass balance and energy equations
67 using obtained water heads and/or flows at nodes ([Rahal et al., 1980](#); [Walski, 1983, 1986 &](#)
68 [Bhave, 1988](#)). However, this approach tends to have a slow convergence rate and is only suitable
69 for handling small-scale problems ([Bhave, 1988](#)).

70 The second category includes explicit models, also known as hydraulic simulation
71 models, which rely on solving an extended set of steady-state equations that include initial
72 equations and additional ones derived from available measurements ([Zanfei et al., 2020](#)). An
73 objective function or cost function is typically applied to minimize the disparities between
74 measured and model-predicted variables ([Savic et al., 2009](#)). However, this method requires a

75 large quantity of observation data to accurately estimate calibration parameters (Walski, 2000).
76 Nevertheless, simplifications of the model should be made to find a reasonable solution.

77 The third category of calibration methods involves implicit models that are generally
78 based on optimization techniques. The calibration variables for these models encompass a broad
79 range of parameters, such as nodal demand and pipe roughness (Wu et al., 2002), or valve status
80 and leak parameters (Lauccelli et al., 2011). A variety of optimization methods have been
81 employed to address the relevant calibration problem, including the general reduced gradient
82 method (Shamir, 1974; Lansley & Basnet, 1991), the Gauss-Newton method (Reddy et al., 1996),
83 the Levenberg-Marquardt method (Liggett & Chen, 1994), the extended complex method of box
84 (Ormsbee, 1989), linear and non-linear programming (Greco & Del Giudice, 1999), the Kalman
85 filtering method (Todini, 1999), and the simulated annealing method (Tucciarelli et al., 1999).
86 However, there are trade-offs and no general guidance exists regarding which optimization
87 technique is preferable for a specific calibration problem.

88 Various optimization techniques have been proposed for model calibration utilizing
89 genetic algorithms (GAs) (Dandy et al., 1996; Savic & Walters, 1995; Vítkovský & Simpson,
90 1997; Tang et al., 1999; Kapelan, 2002; Vítkovský et al., 2000, 2003; Lingireddy & Ormsbee,
91 1998; Meirelles et al., 2017; Zanfei et al., 2020). GAs have been shown to be efficient in
92 assessing sensitivities, managing extensive calibrations, and integrating additional calibration
93 parameter types and constraints into the optimization process. Recently, researchers have
94 explored the use of evolutionary computer techniques to calibrate hydraulic models, with a focus
95 on leakage estimation (Di Nardo et al., 2014; Covelli et al., 2015) and water demand (Do et al.,
96 2016).

97 However, the roughness coefficient is a primary parameter that contributes to uncertainty
98 in model outputs, and different equations may yield vastly different estimates of frictional head
99 losses, depending on the pipe size and water flow rate (Rehan Jamil, 2019; Hashemi et al., 2020).
100 The Darwin Calibrator in the commercial WaterGEMs has been developed utilizing GA to
101 enable the adjustment of model parameters and modification of the roughness of pipe groups and
102 junction demand during the calibration process (Wu, 2004). However, WaterGEM did not
103 account for the spatial characteristics of pipes in WDS calibration.

104 Regarding the previous requirements and limitations, this study proposes an enhanced
105 method that employs Genetic Algorithm to optimize the roughness coefficient while
106 incorporating the spatial factor and actual junction demand in the EPANET hydraulic model.
107 Notably, EPANET is a freely available software that models the water quality and hydraulic
108 behavior of water distribution piping systems (Nallanathel et al., 2018). Furthermore, a case
109 analysis is carried out in the study to illustrate how the proposed technique can enhance the
110 operational effectiveness by minimizing the difference between the simulated and observed
111 values. The proposed method is further compared to WaterGEMs to provides a reliable reference
112 for the design and routing scenario of WDS.

113

114

115

116

117 2 Materials and Methods

118 2.1 Overall concept

119 This study aims to collaborate with an EPANET-based hydraulic model
120 algorithm (Shiu et al., 2022), which is a useful and accessible tool for users to build
121 automated processes and handle critical system parameters, such as nodes, links,
122 demand, properties, pumps, reservoirs, and roughness. The study presents a modified
123 approach for calibrating the roughness coefficient in a hydraulic model using a Graphic
124 User Interface (GUI) and a Genetic Algorithm (GA). GA approach is applied in the field
125 to reduce the difference between the observed and predicted values, and it can be used as
126 a valuable reference for future water supply deployment in emergency situations or for
127 adjusting water supply at monitoring centers. Moreover, the water analysis model can
128 identify leaking pipe sections in the network, thereby improving the maintenance
129 efficiency of the pipe network for the administration.

130 Genetic Algorithms (GAs) are biologically motivated adaptive computer
131 techniques based on natural selection and genetic operators (Wang, 1991; Babovic et al.,
132 1994). These algorithms are often used to solve complex optimization problems (Di
133 Nardo et al., 2014; Do et al., 2016; Mambretti, S. & E. Orsi, 2016; Meirelles et al., 2017;
134 Zanfei et al., 2020). The computing framework in this study begins with data
135 preprocessing, transforming the spatial database of the study area into the initial model,
136 which includes a set of initial roughness coefficients denoted as C. These coefficients are
137 estimated using theoretical or empirical formula, such as the Hazen-Williams equation
138 shown in Equation (1) (Williams et al., 1909), which is an empirical relationship
139 between the flow of water in a pipe and the physical properties of the pipe, as well as the
140 pressure drop caused by friction:

$$141 \quad V = k C R^{0.63} S^{0.54} \quad (1)$$

142 where V is velocity (in ft/s for US units, in m/s for SI units), k is a conversion
143 factor for the unit system (k = 1.318 for US units, k = 0.849 for SI units), R is the
144 hydraulic radius (in ft for US units, in m for SI units), and S is the slope of the energy
145 line (head loss per length of pipe or hf/L).

146 The roughness coefficient C of a pipe is a dimensionless number that depends on
147 the pipe material, and in this study, the pipe roughness is categorized based on the
148 fabrication material, including cast iron, plastic, and stainless steel. The roughness of
149 new cast iron pipes is 130, while the roughness of 20-year-old pipes is 95, and 30-year-
150 old pipes are 82.5. For plastic pipes, regardless of the age, the roughness is set at 150.
151 For stainless steel pipes, the roughness of new riveted steel pipes is 110. The roughness
152 of other pipelines is 100 (Williams et al., 1909).

153 The process of calibration involves adjusting the roughness coefficient value C
154 through EPANET and optimization techniques to minimize the difference between
155 predicted pressures P and measured pressures, resulting in the creation of a corrected
156 INP file for EPANET. Figure 1 illustrates the overall concept, while Equation (2)
157 represents the objective function used for genetic algorithm correction:

158
$$F(x) = \min (\sum_1^n (P - \Delta P)^2) \quad (2)$$

159 The objective function, $F(x)$, is defined as the minimized sum of n th water
160 pressure difference squared, where ΔP represents the actual measured value and P
161 represents the model predicted value. The model predicted value is obtained by adjusting
162 the C value of each pipeline and substituted into EPANET.dll for calculation.
163

164 2.2 The modified GA operation process

165 This research developed a modified GA operation, which consists of three stages
166 as depicted in [Figure 2](#): Data preparation, GA analysis, and Data output. These stages
167 are further explained below:

168 1. Data Preparation:

169 The first stage involves reading the config.ini file to retrieve the initial settings,
170 followed by inputting the water distribution system (WDS) initialized model (input.inp)
171 and water pressure measurements (observation.csv) data for the calculation process. The
172 data is then checked for accuracy before proceeding to the next step. If an error is
173 detected, the calculation process is terminated. The INP file is then read to obtain
174 information of the material types of the pipelines, pipeline diameters, pipeline roughness
175 coefficient (C), and setting the group by diameter and roughness coefficient.

176 2. GA analysis:

177 The GA is initialized, and the roughness coefficient (C) of the pipeline in the
178 input.inp file is automatically imported to the EPANET.dll to perform the analysis. The
179 percentage of pressure difference is then calculated. If new entities are presented, the
180 process calculates fitness, performs selection, crossover, mutation, creates a new
181 generation, and stores the optimized solution in the INP file.

182 3. Data Output:

183 The results include three types: reports in TXT format, fitting curves in PNG
184 format, and statistical charts in PNG format.

185 2.3 GA Graphic User Interface Design

186 To enhance the efficiency and ease of use of the calibration software, a graphic
187 user interface (GUI) was developed using a GA, called WaterCali in this study. The
188 interface is divided into six sections: the input area, GA parameter settings area, upper
189 and lower limits of roughness, pipeline grouping settings area (with a focus on the
190 spatial area), calibration result display area, and function key area. The WaterCali
191 interface is illustrated in [Figure 3](#) and offers a simple and intuitive user experience.

192

193

194

195 This study proposes four group methods for setting groups in WaterCali,
 196 particularly in spatial groups. In Taipei, for example, the elevation ranges from 0 to 1177
 197 meters. The user can input a GeoJSON file that contains area geometry to restrict the
 198 roughness coefficient (C) to the same area as follows.

```
199
200 “{ "type": "FeatureCollection",
201     "name": "A",
202     "crs": { "type": "name", "properties": { "name": "urn:ogc:def:crs:EPSG::3826" } },
203     "features": [
204         { "type": "Feature", "properties": { "id": 0, "area": 131874.60656700001, "perimeter":
205         1367.29384 }, "geometry": { "type": "Polygon", "coordinates": [ [ [ 300076.488, 2773317.927 ],
206         [ 299863.84, 2773330.234 ], [ 299770.886, 2773347.906 ], [ 299716.224, 2773429.392 ], [
207         299843.986, 2773650.023 ], [ 300018.272, 2773651.079 ], [ 300122.724, 2773642.446 ], [
208         300163.252, 2773613.56699999981 ], [ 300200.169, 2773517.413 ], [ 300207.555, 2773403.838
209         ], [ 300185.121, 2773370.367 ], [ 300076.488, 2773317.927 ] ] ] } } ]
210     } ”
```

211
 212 Once the calibration process is finished, the outcomes are saved in the output
 213 folder located in the data directory, depicted in Figure 4. These outcomes encompass
 214 pressure data, illustrated in Figure 5, INP files for each generation, pipeline groups, and
 215 statistical charts and implementation reports presenting the results of each iteration.

217 3 Introduction of case area

218 3.1 Introduction of case area

219 The case study was conducted at Taipei Water Department's Zhonghe and
 220 Yonghe Division. The Zhonghe Booster Station is the primary water supply facility for
 221 the Zhonghe District and Yonghe Division, where the northern side is a relatively low-
 222 pressure area, and the water source is derived from two branch lines of the Zhitan Water
 223 Treatment Plant, as illustrated in Figure 6. Table 1 provides some essential details of
 224 Taipei Water Department's Zhonghe and Yonghe Division.

225
 226 **Table 1.** Basic information of study area

Division	Pipe Length (Km)		Valve	Hydrant	Meter	Booster Station	Tank Volume(t)	Monitoring Point
	Water-Distribution	Water-Service						
Zhonghe	256	156	3,690	2,542	20,943	1	30,222	5
Yonghe	143	108	2,552	1,421	15,554			5

227 3.2 Model establishment

228 The WISE (Water Intelligent System of Enterprise) platform of the Taipei Water
229 Department is currently in use, which allows users to select an area on the map and
230 choose the water demand distribution model, then export the model for further analysis.
231 The resulting model can be opened in EPANET for analysis, as demonstrated in [Figure](#)
232 [7](#). Following the aforementioned processing and calculations, the input parameter table
233 for the selected area can be generated, resulting in an EPANET 2.X input file (*.inp).
234 The INP file for the Zhonghe and Yonghe Division was used to compare the collected
235 station and equipment data.

236

237 3.3 SCADA data for pre-processing

238 Hydraulic model calibration is required to process a large amount of Supervisory
239 Control and Data Acquisition (SCADA) data, including the pressure and flow
240 measurements from field pump stations. The SCADA procedures in this study was
241 organized as follows:

- 242 1. Collecting pump station data: collecting pump station data manually according to the
243 target area for the calibration. To facilitate subsequent data selection and organization,
244 the recommended data collection interval is once per minute.
- 245 2. Calculate the actual water requirement of the pipe network: using Microsoft Excel
246 (Microsoft, Redmond, WA, USA) for data calculation and organization. The data
247 required for organization and calculation are inputted into the EPANET to use its
248 built-in formulas for calculation.
- 249 3. Determine the time slot of the maximum water requirement: From the previous
250 calculation results, the maximum value of water amount is identified, then the
251 corresponding time slot is used for EPANET at single time period simulation.
- 252 4. Obtain the data of all pump stations and monitoring points of the corresponding time
253 slot: because the basis for single time period simulation has been identified and data of
254 all pump stations can be established in the EPANET, including the inflows and
255 outflows, and pressures. Thus, the pressure values of the monitoring points at the
256 corresponding time slot are listed for comparison and model modification, as shown in
257 [Figure 8](#).

258

259 3.4 Water Pressure Measurements

260 According to suggestion of [Shiu et al. \(2022\)](#), the total measured points of this
261 study is set to 140 to satisfy the measured quantity which is at least 30% of the model
262 length(km) as following [Equation \(3\)](#):

$$263 \text{ Pipe length}(km) \text{ of the Model} * 0.3 \leq \text{Measured Points } (\Delta P) \quad (3)$$

264 In addition, the 140 measured points should be uniformly located in the water
265 supply zone to understand the distribution of the water supply pressure. In order to

266 prevent the measured error by unexpected valve closing, the measured points were
 267 randomly separated into two groups, red and green triangulars as shown in Figure 9.
 268 Each point was then installed with a pressure sensor to retrieve data more than 48 hours,
 269 the frequency of pressure measurement data recorded once per minute , as shown in
 270 Figure 10.

271 The time series display the pattern of two groups, as shown in Figure 11(A) and
 272 Figure 11(B). In this case study, the high peak of measured data was about 23:00 and the
 273 low peak is about 22:00. Measuring point No. 058 and 065 have a sharp drop in pressure
 274 at 2021/12/28 at 22:00, as shown in Figure 12, because of the large water consumption
 275 at the same time. It came back to normal suddenly. The water consumption recorded by
 276 the water meter at 22:00 on 2021/12/28 was 51~73% higher than the water consumption
 277 at 22:00 on 2021/12/29.
 278

279 3.5 Parametric results for GA

280 The validated paramters in GA are categorized into three types, as shown in
 281 Table 2 below. For the first type, the generation has been set as 100 and the Roughness
 282 Coefficient C as between 35 and 300 for testing the water head loss being reduced and
 283 reflected in C. In the second type, the generation was 50 and lies between 50 and 150 for
 284 testing the GA performance. In the third type, the generation is set 50 and C between 70
 285 and 150 for imiting the value of C to get better results. Type I and II were used to
 286 compare the generation and GA performance, and Type II and III were used for a C
 287 comparison. It reflects that imiting the value of C can not get better results.

288 Figure 13 shows that Type I is fit in 45 generations and the mean error rate is
 289 about 11.759%. For Type II, the fitness is shown in 20 generations and the mean error
 290 rate is about 11.765%. In Type III, the result is also fit in 20 generations and the mean
 291 error rate is about 11.844%, as shown in Figure 13. The qualified point in Type I with
 292 113, Type II with 114, and Type III with 110. After comparing with Type I and II, 50
 293 generation is enough for using and comparing with Type II and III shows that the C
 294 between 50 and 150 is better.

295 **Table 2.** Scenerio settings for GA

Variable	Type I	Type II	Type III
Population	1,000	1,000	1,000
Generation	100	50	50
Rate Of Crossover	0.8	0.8	0.8
Rate Of Mutation	0.08	0.08	0.08
Proportion Of Optimal	0.1	0.1	0.1
Roughness Coefficient	$35 \leq C \leq 300$	$50 \leq C \leq 150$	$70 \leq C \leq 150$
Qualified Point	113	114	110

* If the initial Roughness Coefficient (C) > 140, it will not be modify in GA model.

297 **4 Results**

298 4.1 Simulation Results before GA Roughness Optimization

299 [Figure 14](#) shows the distribution of the simulated water pressure with the
300 previous SCADA pre-processing before the Roughness Coefficient C optimization.
301 According to the statistical results shown in [Table 3](#), out of the 140 water pressure
302 measurement points in the Zhonghe and Yonghe Divisions, 64 points have a pressure
303 difference of less than 0.1 kg/cm², 44 points have a difference between 0.1 to 0.2
304 kg/cm², 18 points are between 0.2 to 0.3 kg/cm², 8 points are between 0.3 to 0.4 kg/cm²,
305 and 6 points have a difference greater than 0.4 kg/cm².

306 Out of the total, 112 points have a pressure error within ±20%, which accounts
307 for 80% of the total. The area with the largest difference from the actual measured
308 pressure is primarily located at the end of the pipeline, as shown in [Figure 15](#). The
309 pressure at the end of the pipeline is typically lower than in other areas, which causes an
310 obvious difference error.

311 **Table 3.** Statistics of pressure difference before calibration

Water pressure Difference (kg/cm ²)	Count	Percentage (%)	Error (%)	Count	Percentage (%)
< 0.1	64	45.7	10	57	40.7
0.1~0.2	44	31.4	10-20	55	39.3
0.2~0.3	18	12.9	More than 20	28	20.0
0.3~0.4	8	5.7			
More than 0.4	6	4.3			

312

313 4.2 Simulation Results after Roughness Optimization

314 Table 4 displays the simulation results roughness optimization. Among the 140
315 water pressure measurement points, 75 points have a pressure difference of less than 0.1
316 kg/cm², 39 points are between 0.1~0.2 kg/cm², 18 points are between 0.2~0.3 kg/cm², 1
317 point is between 0.3~0.4 kg/cm², and 7 points are above 0.4 kg/cm².

318 The error within 20% is observed in 114 points, accounting for 81.4% of the
319 total, and the error of less than 10% increased from 57 points to 70 points, which
320 suggests a significant improvement in overall pressure difference, as shown in [Figure 15](#).
321 The points with a larger error are primarily located at the end of the pipeline.

322 The absolute value of the pressure difference and the error at each point are
323 closer to the lower range. The calculated correlation coefficient between the mean value
324 observed and the simulated pressure was 0.9, which is considered good compared to the
325 research by [Kepa \(2021\)](#). Based on the calibration, the developed EPANET-GA model
326 was deemed acceptable and represented a reliable representation of the tested water
327 supply network.

328 **Table 4.** Statistics of pressure difference after roughness optimization

Water pressure Difference (kg/cm ²)	Count	Percentage (%)	Error (%)	Count	Percentage (%)
< 0.1	75	53.6	10	70	50
0.1 ~ 0.2	39	27.9	10-20	44	31.4
0.2 ~ 0.3	18	12.8	More than 20	26	81.4
0.3 ~ 0.4	1	0.7			
> 0.4	7	5.0			

329

330 4.3 Comparison with WaterGEMs

331 To assess the reliability and effectiveness of the proposed method, this study
 332 used both the EPANET-GA and WaterGEMs simulation results with those obtained
 333 from actual measured water pressures. WaterGEMs is a comprehensive and user-
 334 friendly decision-support tool for water distribution networks provided by Bentley. This
 335 commercial software is well known to improve the operational strategies of decision
 336 makers, enhance the model-building process, and effectively manage local models (Wu
 337 et al., 2004). Table 5 shows the pressure difference between EPANET-GA after
 338 calibration and WaterGEMs. The results indicate that 112 points have an error within
 339 20%, which accounts for 80% of the total, and 57 points have an error less than 10%.
 340 EPANET-GA outperformed WaterGEMs in terms of accuracy.

341 **Table 5.** Comparison of prediction errors of WaterGEMs and EPANET-GA

WaterGEMs			EPANET-GA		
Error(%)	Count	Percentage(%)	Error(%)	Count	Percentage(%)
<10	64	45.7	<10	71	50.0
10~20	48	34.3	10~20	45	31.4
> 20	28	20.0	> 20	24	18.6

342

343 4.4 Assessment of longterm simulation

344 Based on the previous section's analysis, it was found that the areas with
 345 significant pressure differences before model calibration were mainly located at the end
 346 of the pipeline, as indicated in Figure 17. To assess the reliability of the EPANET-GA
 347 model for long-term simulation, the simulation results were compared with the
 348 monitoring points using 24-hour data, as shown in Figure 18. The EPANET-GA model's
 349 mean error rate after calibration for all monitoring points in 24 hours was 8.93%.

350 Figure 19 shows a comparison of the pressure difference between EPANET-GA
 351 after calibration with WaterGEMs, with 10 monitoring points used for comparison. The
 352 results indicate that the EPANET-GA method has slightly better performance with an

error rate of 8.93%, compared to WaterGEMs with an error rate of 9.00%. When the monitoring points are near the Pump Station, they tend to yield better simulation results with an error rate of less than 10%. However, larger error values can still be observed at the end of the pipe network.

5 Discussion

This technical article presents three primary topics of discussion. Firstly, EPANET-GA highlights the importance of adjusting the valve setting for calibrating the water distribution network model. It is crucial to match the local settings and measurement conditions obtained from SCADA before initiating GA optimization to achieve optimal simulation results and streamline the model checking process. Failure to do so may lead to significant effort being expended to identify problems in the simulation, resulting in mismatched outcomes.

Secondly, measurement points should be randomly selected in a normal distribution within the pipe network and divided into at least two groups to mitigate the impact of the pipe network's operations, as previously mentioned. The measurement duration must be at least 48 consecutive hours.

Thirdly, the GA process varies between WaterCali and WaterGEMs. While WaterCali employs random crossover and mutation techniques, WaterGEMs limits user control of the random variable and transforms it using Fast Messy Genetic Algorithm. WaterCali also incorporates the spatial factor in the calibration process, making it better suited for real-world scenarios and simulations.

6 Conclusions and Suggestions

The proposed methodology involves combining the genetic algorithm (GA) with the EPANET.dll water analysis library to create EPANET-GA, which enables identification of the optimal solution that aligns with measured data. The roughness coefficient is adjusted by the GA through iterations of selection, crossover, and constant mutation. To validate the efficiency of the pipeline network model and calibration process, results were compared with SCADA monitoring points at Zhonghe and Yonghe Division. The hydraulic model's preliminary analysis results indicate a reasonable distribution of water pressure calculated by the Zhonghe and Yonghe Division model. The results demonstrate a strong correlation coefficient of 0.9 between the simulated and measured data, a mean error rate of only 8.93% compared to 24-hour monitoring data, and superior performance compared to WaterGEMs. EPANET-GA can rapidly identify a range of solutions, not just a single optimal solution.

The case of the water pressure calculated by EPANET-GA in Zhonghe and Yonghe Division model indicates that the analysis model could be used in future work programs, such as Taipei Water Department's Shilin and Beitou Division, aiding engineers in decision-making and providing cost-effective solutions. However, the traditional EPANET software currently lacks model calibration functions, and a plug-in solver is required for operation, which is inconvenient for ordinary users. Given that commercial software can be expensive, this study provide WaterCali plugin to share with interested parties requiring reliable water distribution network calibration. Users can refer to the proposed processes and procedures to quickly construct a preliminary hydraulic analysis model and adjust parameters as required for future models.

395

396 **Acknowledgments**

397 This research was supported in part by the Taipei Water Department, Taiwan, ROC.
398 Contract No. 10937017S30.

399

400 **References**

401 Babovic, V., Wu Z. & Larsen, L.C. (1994). Calibrating hydrodynamic models by means of
402 simulated evolution, *Hydroinformatics* 94, 193-200.

403 Balla, M. C. & Lingireddy, S. (2000). Distributed genetic algorithm model on network of
404 personal computers. *Journal of Computing in Civil Engineering* 14 (3), 199–205.

405 Bhave, P. R. (1988). Calibrating water distribution network models. *Journal of environmental
406 engineering* 114 (1), 120–136.

407 Covelli, C., Cozzolino, L., Cimorelli, L., Della Morte, R., Pianese, D. (2015) A model to
408 simulate leakage through joints in water distribution systems. *Water Supply*, 15, 852–863.

409 Dandy, G.C., Simpson, A.R. and Murphy, L.J. (1996). An improved genetic algorithm for pipe
410 network optimisation. *Water Resources Research*, Vol. 32, No. 2, Feb., 449–458.

411 Di Nardo, A., Di Natale, M., Gisonni, C. & Iervolino, M. (2014). A genetic algorithm for
412 demand pattern and leakage estimation in a water distribution network. *J. Water Supply Res.
413 Technol.* 64, 35–46.

414 Do, N.C., Simpson, A.R., Deuerlein, J.W. & Piller, O. (2016). Calibration of water demand
415 multipliers in water distribution systems using genetic algorithms. *J. Water Resour. Plan.
416 Manag.* 142, 04016044.

417 Goldberg, D. E. (1989). *Genetic Algorithms in Search, Optimization and Machine Learning*,
418 Addison-Wesley Longman Publishing, Massachusetts.

419 Greco, M. & Del Giudice, G. (1999). New approach to water distribution network calibration.
420 *Journal of Hydraulic Engineering* 125 (8), 849–854.

421 Hazen-Williams Coefficients, Engineering ToolBox, retrieved 7 October 2012

422 https://www.engineeringtoolbox.com/hazen-williams-coefficients-d_798.html

423 Hashemi, S., Filion, Y., Speight, V. & Long, A. (2020). Effect of Pipe Size and Location on
424 Water-Main Head Loss in Water Distribution Systems. *Journal of Water Resources
425 Planning and Management* 146(6): 06020006.

426 Holland, J. H. (1975). *Adaptation in Natural and Artificial System*. Ann Arbor. The University of
427 Michigan Press.

428 Kapelan, Z. (2002). *Calibration of Water Distribution System Hydraulic Models*. Ph.D. thesis,
429 School of Engineering and Computer Science, University of Exeter, Exeter, UK.

430 Kapelan, Z., Savic, D. A. & Walters, G. A. (2004). Incorporation of prior information on
431 parameters in inverse transient analysis for leak detection and roughness calibration. *Urban*
432 *Water* 1(2), 129–143.

433 Kepa, U. (2021) Use of the hydraulic model for the operational analysis of the water supply
434 network: a case Study. *Water*, 2021. 13, 326.

435 Lansey, K. E. & Basnet, C. (1991). Parameter estimation for water distribution networks.
436 *Journal of Water Resources Planning and Management* 117 (1), 126–144.

437 Laucelli, D., Berardi, L., Giustolisi, O., Vamvakeridou-Lyroudia, L.S., Kapelan, Z., Savic, D. &
438 Barbaroand, G. (2011). Calibration of Water Distribution System Using Topological
439 Analysis. In *Water Distribution Systems Analysis; American Society of Civil Engineers:*
440 Tucson, AZ, SA, 2011; pp. 1664–1681.

441 Liggett, J. A. & Chen, L. C. (1994). Inverse transient analysis in pipe networks. *Journal of*
442 *Hydraulic Engineering* 120 (8), 934–955.

443 Lingireddy, S. & Ormsbee, L. E. (1998). *Optimal Network Calibration Model Based on Genetic*
444 *Algorithms*. Tech. rep., University of Kentucky, USA.

445 Michalewicz, Z. (1992). *Genetic Algorithms + Data Structures = Evolutionary Programs*,
446 Springer Berlin, Heidelberg.

447 Meirelles, G., Manzi, D., Brentan, B.M., Goulart, T., Junior, E.L. (2017) Calibration Model for
448 Water Distribution Network Using Pressures Estimated by Artificial Neural Networks.
449 *Water Resource Management*. 31, 4339–4351. <https://doi.org/10.1007/s11269-017-1750-2>

450 Mambretti, S. and E. Orsi (2016). Optimizing Pump Operations in Water Supply Networks
451 Through Genetic Algorithms. *Journal AWWA* 108(2): E119-E125.

452 Nallanathel M., Ramesh B., Santhosh A. P. (2018). Water distribution network design using
453 EPANET A case study. *International Journal of Pure and Applied Mathematics*. Volume
454 119 No. 17, 1165-1172

455 Ormsbee, L. E. & Wood, D. J. (1986). Explicit network calibration. *Journal of Water Resources*
456 *Planning and Management* 112 (2), 166–182.

457 Ormsbee, L. E. (1989). Implicit network calibration. *Journal of Water Resources Planning and*
458 *Management* 115 (2), 243–257.

459 Rahal, C. M., Sterling, M. J. H. & Coulbeck, B. (1980). Parameter tuning for simulation models
460 of water distribution networks. *In: Institution of Civil Engineers*. No. 69. pp. 751–762.

461 Reddy, P. V. N., Sridharan, K. & Rao, P. V. (1996). WLS method for parameter estimation in
462 water distribution networks. *Journal of Water Resources Planning and Management* 122
463 (3), 157–164.

464 Rehan Jamil (2019). Frictional head loss relation between Hazen-Williams and Darcy-Weisbach
465 equations for various water supply pipe materials. *International Journal of Water* 13(4):
466 333-347.

467 Sitzenfrei, R., Wang, Q., Kapelan, Z., & Savić, D. (2020). Using complex network analysis for
468 optimization of water distribution networks. *Water Resources Research*, 56,
469 e2020WR027929. [https://doi.org/ 10.1029/2020WR027929](https://doi.org/10.1029/2020WR027929)

470 Savic, D.A. and Walters, G. A. (1994). Evolution programs in optimal design of hydraulic
471 networks, in *Adaptive Computing in Engineering Design and Control '94*, edited by I.C.
472 Parmee, University of Plymouth, Plymouth, UK, pp. 146-150.

473 Savic, D. A. & Walters, G. A. (1995). *Genetic Algorithm Techniques for Calibrating Network*
474 *Models*. Tech. Rep. 95/12, Centre for Systems and Control Engineering, University of
475 Exeter, UK.

476 Savic, D. A., Kapelan, Z. S. & Jonkergouw, Philip M. R. (2009). Quo vadis water distribution
477 model calibration?. *Urban Water Journal*. 6. 3-22. 10.1080/15730620802613380.

478 Shamir, U. (1974). Optimal design and operation of water distribution systems. *Water Resources*
479 *Research* 10 (1), 27–36.

480 Shiu, C.-C., Chiang, T. & Chung, C.-C. (2022). A modified hydraulic model algorithm based on
481 integrating graph theory and GIS database. *Water* 2022, 14, 3000.
482 <https://doi.org/10.3390/w14193000>

483 Tang, K., Karney, B., Pendlebury, M. & Zhang, F. (1999). Inverse transient calibration of water
484 distribution systems using genetic algorithms. In: Savic, D. A., Walters, G. A. (Eds.), *Water*
485 *Industry Systems: Modelling and Optimization Applications*. Vol. 1. Exeter, UK, pp. 317–
486 326.

487 Todini, E. (1999). Using a kalman filter approach for looped water distribution network

488 calibration. In: Savic, D. A., Walters, G. A. (Eds.), *Proceedings Water Industry Systems:*
489 *Modelling and Optimization Applications*. Vol. 1. University of Exeter, UK, pp. 327–336.

490 Tucciarelli, T., Criminisi, A. & Termini, D., (1999). Leak analysis in pipeline systems by means
491 of optimal valve regulation. *Journal of Hydraulic Engineering* 125 (3), 277–285.

492 Vítkovský, J. P. & Simpson, A. R. (1997). *Calibration and Leak Detection in Pipe Networks*
493 *Using Inverse Transient Analysis And Genetic Algorithms*. Tech. Rep. R 157, Department of
494 Civil and Environmental Engineering, University of Adelaide.

495 Vítkovský, J. P., Simpson, A. R. & Lambert, M. F. (2000). Leak detection and calibration using
496 transients and genetic algorithms. *Journal of Water Resources Planning and Management*
497 126 (4), 262–265.

498 Vítkovský, J. P., Liggett, J.A., Simpson, A. R. & Lambert, M. F. (2003). Optimal measurement
499 site locations for inverse transient analysis in pipe networks, *Journal of Water Resources*
500 *Planning and Management* 129 (6), 480–492.

501 Williams, G. Stewart., Hazen, A. (1909). Hydraulic tables: the elements of gagings and the
502 friction of water flowing in pipes, aqueducts, sewers, etc. as determined by the Hazen and
503 Williams formula and the flow of water over sharp-edged and irregular weirs, and the
504 quantity discharged, as determined by Bazin's formula and experimental investigations upon
505 large models. 2d ed., New York: J. Wiley & sons.

506 Walski, T. (1983). A technique for calibrating network models. *Journal of Water Resources*
507 *Planning and Management* 109 (4), 360–372.

508 Walski, T. M. (1986). Case study: pipe network model calibration issues. *Journal of Water*
509 *Resources Planning and Management* 112 (2), 238–249.

510 Walski, T. M. (2000). Model calibration data: the good, the bad, and the useless, *Journal-*
511 *American Water Works Association*, 92 (1), 94- 99.

512 Wang, Q.J. (1991). The genetic algorithm and its application to calibrating conceptual rainfall-
513 runoff models, *Water Resources Research*, Vol. 27, No. 9, 2467-2471.

514 Wu, Z.Y., Walski, T., Mankowski, R., Herrin, G., Gurrieri, R. & Tryby, M. (2002). Calibrating
515 water distribution model via genetic algorithms. In Proceedings of the 2002 AWWA
516 IMTech Conference, Kansas City, MO, USA, 14–17 April 2002.

517 Wu Z.Y., Arniella E. F. & Gianella E. (2004). Darwin Calibrator - Improving Project
518 Productivity and Model Quality for Large Water Systems. *Journal-American Water Works*

519 *Association*, 96(10), 27-34. <https://doi.org/10.1002/j.1551-8833.2004.tb10715.x>

520 Zanfei, A., Menapace, A., Santopietro, S. & Righetti, M. (2020). Calibration procedure for water
521 distribution systems: comparison among hydraulic models. *Water* 2020, 12, 1421.
522 <https://doi.org/10.3390/w12051421>

523

Figure 1. The proposed EPANET-GA model calibration work flow.

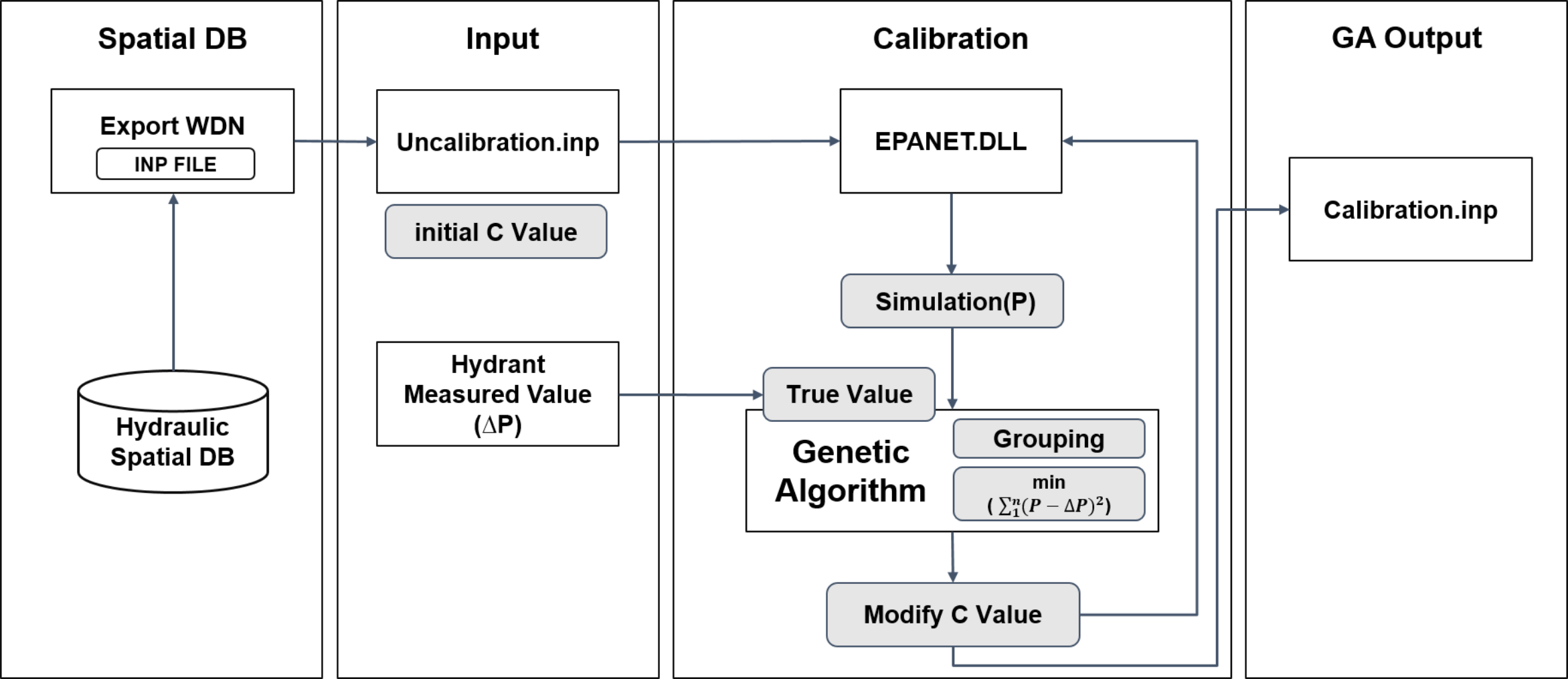
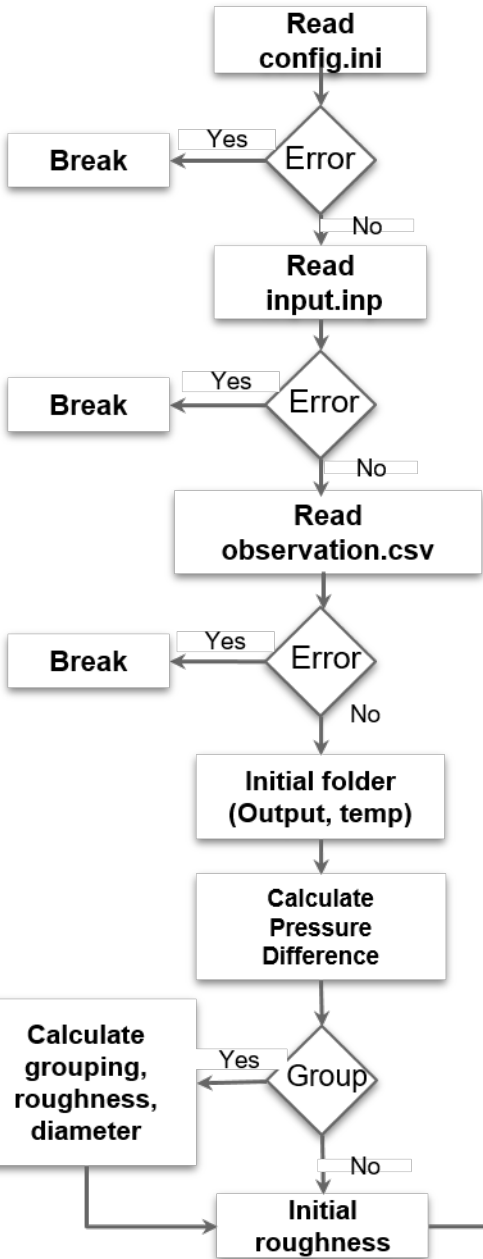
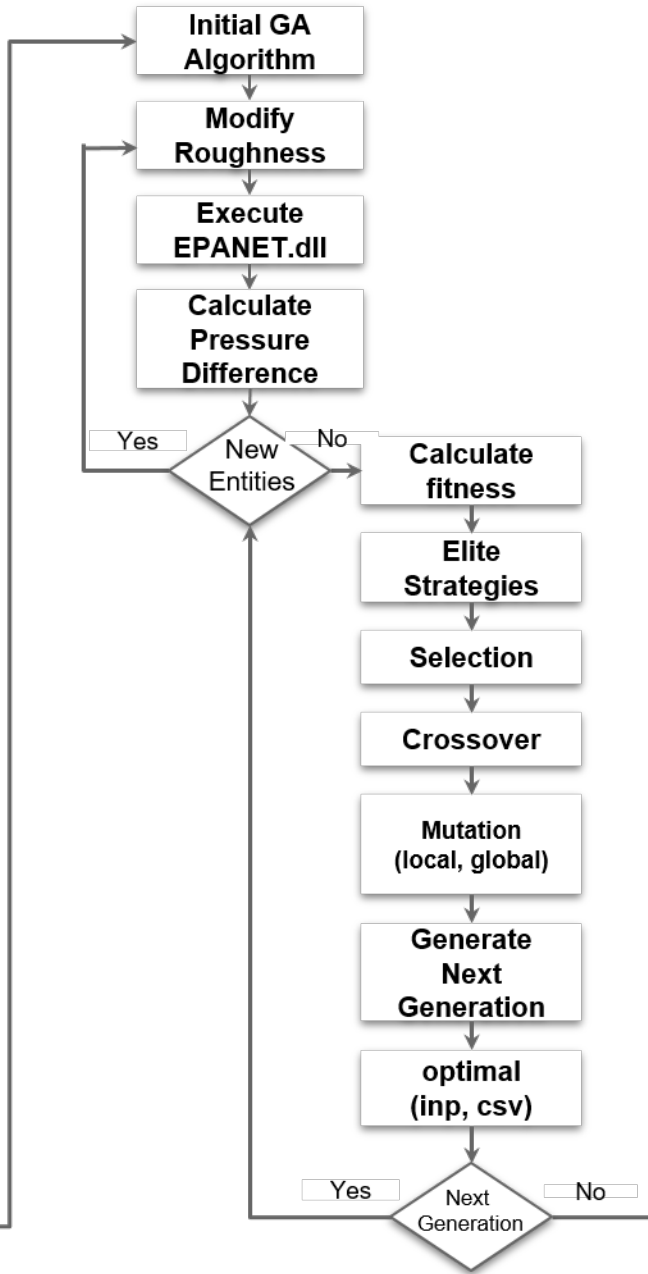


Figure 2. The proposed calibration procedures with GA and EPANET.

Data Preparation



GA Analysis



Data Output

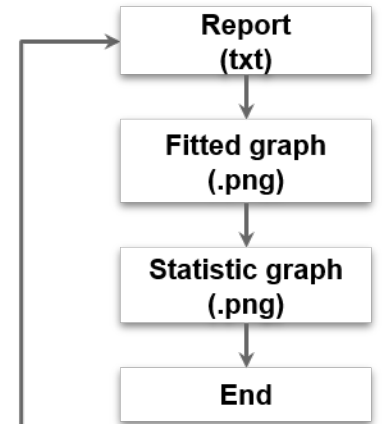


Figure 3. WaterCali graphic user interface (GUI).

WaterCali

Help About

DATA INPUT

開啟檔案
開啟檔案

待校正 inp 檔案 D:\Users\63323\Desktop\WaterCali\data\input\input.inp

實際量測值資料 (格式請參考範例) D:\Users\63323\Desktop\WaterCali\data\input\observation.csv

人口數 (建議 300~1000)	1000
世代數 (建議 30~100)	30
交配機率 (建議 $0.6 < x < 1$)	0.8
突變機率 (建議 $0.01 < x < 0.08$)	0.08
菁英佔比 (建議 $0.01 < x < 0.1$)	0.1
數值 \geq 該數值將不進行校正	140
管線摩擦係數不可低於	50
管線摩擦係數不可高於	200

不分組

自動分組 共 326 組

客製化分組

區域分組

點我下載管線分組清單

執行時間：2022-03-03-09-26-15

```

2022-03-03 09:26:18 - [ 第 0 世代 ]
2022-03-03 09:26:18 - 平均壓力誤差(%)：14.226
2022-03-03 09:36:19 - [ 第 1 世代 ]
2022-03-03 09:36:19 - 平均壓力誤差(%)：13.28
2022-03-03 09:45:29 - [ 第 2 世代 ]
2022-03-03 09:45:29 - 平均壓力誤差(%)：12.854
2022-03-03 09:54:54 - [ 第 3 世代 ]
2022-03-03 09:54:54 - 平均壓力誤差(%)：12.719
2022-03-03 10:04:37 - [ 第 4 世代 ]
2022-03-03 10:04:37 - 平均壓力誤差(%)：12.634
2022-03-03 10:14:25 - [ 第 5 世代 ]
2022-03-03 10:14:25 - 平均壓力誤差(%)：12.514
2022-03-03 10:24:03 - [ 第 6 世代 ]
2022-03-03 10:24:03 - 平均壓力誤差(%)：12.329

```

世代數	平均壓力誤差(%)
0	14.226
1	13.28
2	12.854
3	12.719
4	12.634
5	12.514
6	12.329

run clear exit

Inp
Observation Data

GA Coefficients

Roughness Upper And
Lower Limits

Group Type Setting

Result Display
Area

Function Key

Figure 4. WaterCali output files.

 elite —————● **Calibration result of node**

 inp —————● **Calibration result of INP**

 custom_cluster.csv —————● **Group Of Pipeline**

 fit_curve_graph.png —————● **Fitting Curve**

 report.txt —————● **Calibration Report**

Figure 5. WaterCali water pressure calculations in an output Excel file.

新細明體 12 A A 通用格式 設定格式化的條件 插入 格式化為表格 刪除 格式 儲存格樣式 儲存格 編輯

B I U 中 對齊方式 數值 樣式 儲存格 編輯

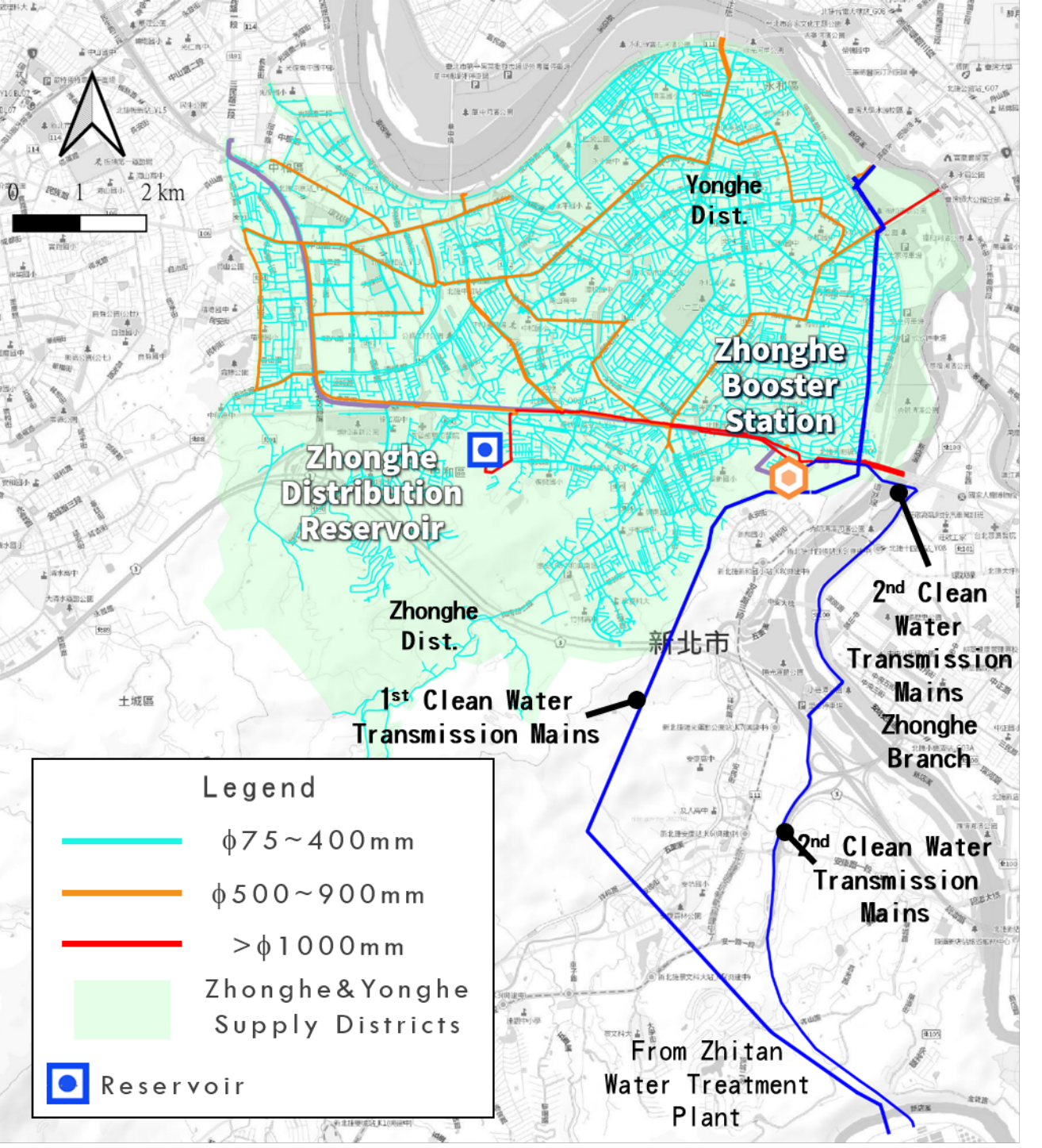
Observation Simulation Difference Error

Value Value Value Percentage

(kg/cm²) (M) (M) (%)

	A	B	Value	Value	Value	Percentage	H	I	J	
	id	node_id	pressure (kg/cm ²)	actual_pressure (M)	simulation_pressure (M)	pressure_error (M)	pressure_error_percentage (%)			
1	id	node_id	pressure	actual_pressure	simulation_pressure	pressure_error	pressure_error_percentage			
2	1	WPU63012006986_1_E	1.716	17.16	17.41237831	0.252378311	1.470736079			
3	2	WPU63011019419_E	1.451	14.51	15.53568459	1.025684586	7.068811754			
4	3	WPU63012017105_E	1.265	12.65	11.14365959	1.506340408	11.90782931			
5	4	WPU63011019166_E	1.721	17.21	15.87079048	1.339209518	7.781577678			
6	5	WPU63011019500_E	1.03	10.3	12.03906822	1.739068222	16.8841575			
7	6	WPU63012005710_E	1.716	17.16	17.08580971	0.074190292	0.432344361			
8	7	WPU63012005726_E	2.078	20.78	18.90875626	1.871243744	9.005022829			
9	8	WPU63012000693_E	2.13	21.3	18.43276024	2.867239761	13.46121954			
10	9	WPU63012005732_E	1.657	16.57	16.07526016	0.494739838	2.985756413			
11	10	WPU63012005788_E	2.353	23.53	20.45352173	3.076478271	13.07470579			
12	11	WPU63012005795_E	1.961	19.61	18.21741867	1.392581329	7.101383627			
13	12	WPU63011012524_E	1.549	15.49	15.6606493	0.1706493	1.101673981			
14	13	WPU63011013871_E	1.118	11.18	11.18326855	0.003268547	0.029235662			
15	14	WPU63011014727_E	4.343	43.43	41.1795845	2.250415497	5.181707338			
16	15	WPU63011012117_E	1.451	14.51	14.29672623	0.213273773	1.469839926			
17	16	WPU63011011999_E	1.549	15.49	13.59189129	1.898108711	12.25376831			
18	17	WPU63011012110_E	1.48	14.8	13.65445614	1.145543861	7.740161226			
19	18	WPU63011013304_E	0.84	8.4	9.222138405	0.822138405	9.787361962			
20	19	WPU63011010816_E	1.49	14.9	13.50214386	1.39785614	9.381584833			

Figure 6. Water supply and pipeline distribution of the Zhonghe and Yonghe Divisions.



Legend

- $\phi 75 \sim 400$ mm
- $\phi 500 \sim 900$ mm
- $> \phi 1000$ mm
- Zhonghe & Yonghe Supply Districts

● Reservoir

From Zhitan
Water Treatment
Plant

2nd Clean
Water
Transmission
Mains
Zhonghe
Branch

2nd Clean Water
Transmission
Mains

Zhonghe
Distribution
Reservoir

1st Clean Water
Transmission Mains

Yonghe
Dist.

Zhonghe
Booster
Station

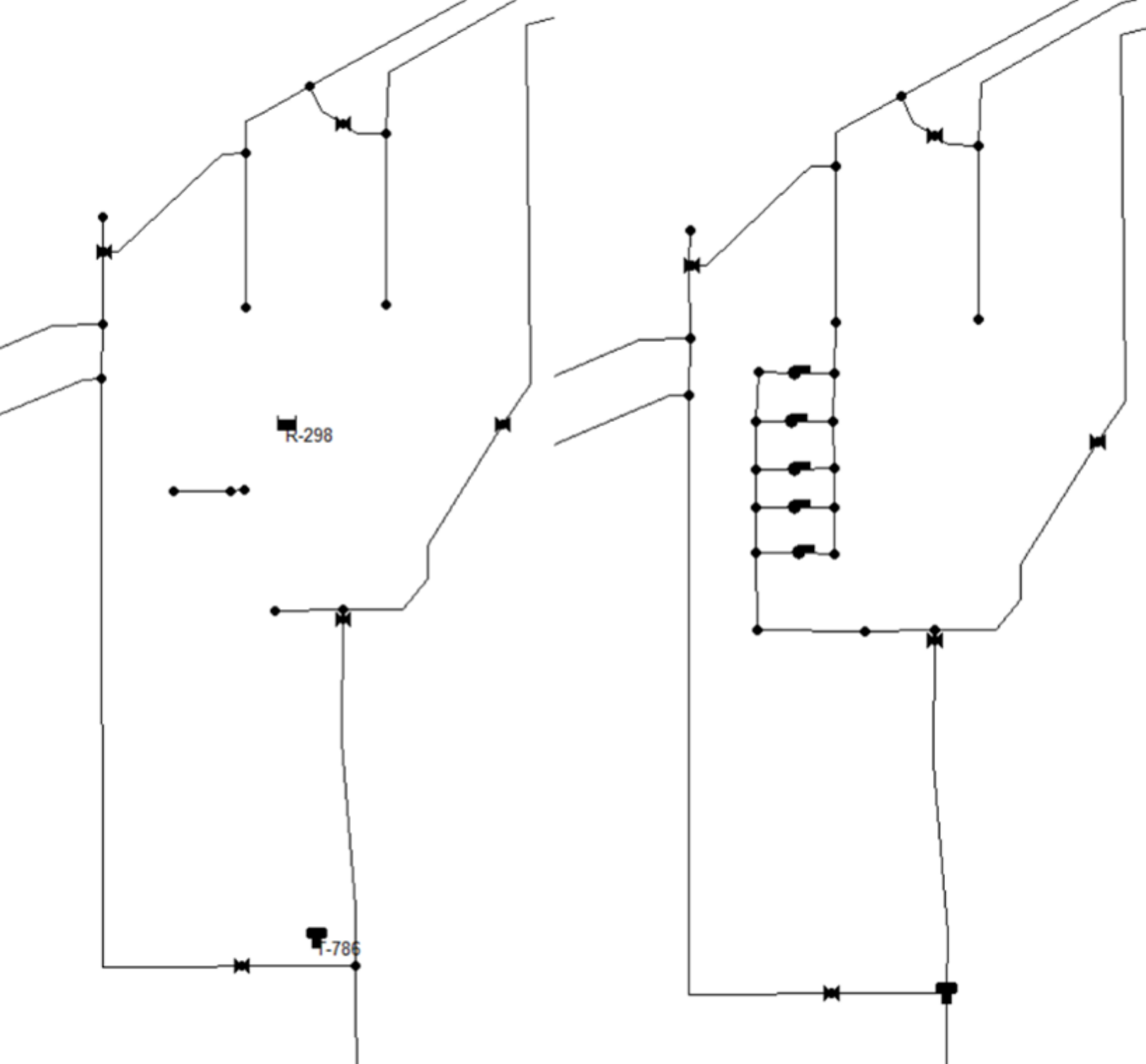
Zhonghe
Dist.

新北市

Figure 7. INP network of the Zhonghe and Yonghe Divisions.



Figure 8. Setting Variables and links of Pump in EPANET.



Curve Editor

Curve ID: Description:

Curve Type: Equation:

Flow	Head
125000	30

Buttons: Load... Save... OK Cancel Help

Curve Editor

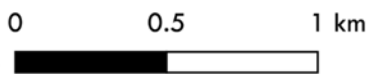
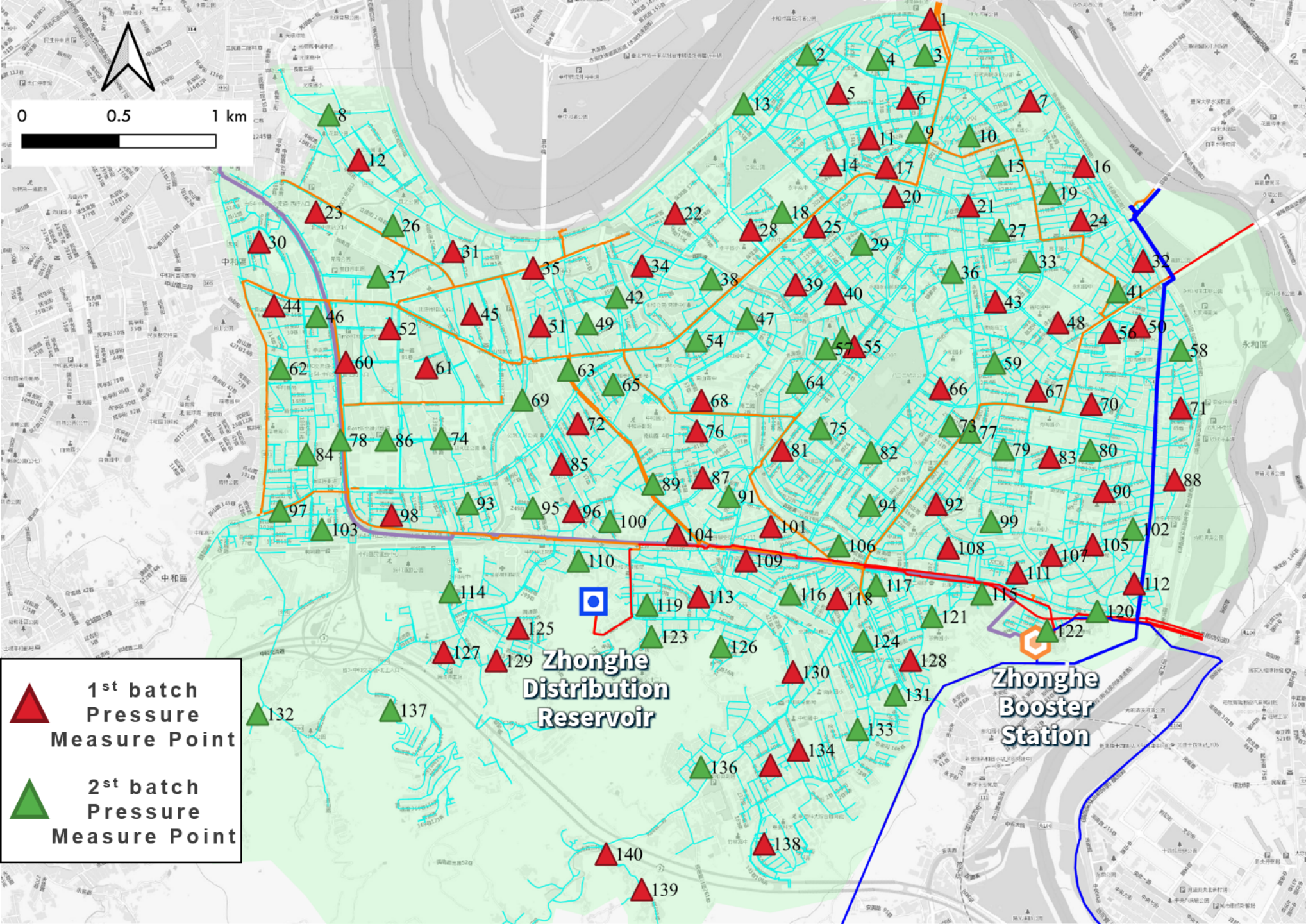
Curve ID: Description:

Curve Type: Equation:

Flow	Head
135000	20

Buttons: Load... Save... OK Cancel Help

Figure 9. Distribution of measurement points in the Zhonghe and Yonghe Divisions.



-  1st batch Pressure Measure Point
-  2nd batch Pressure Measure Point

**Zhonghe
Distribution
Reservoir**

**Zhonghe
Booster
Station**

Figure 10. Work flow of installing a pressure sensor.



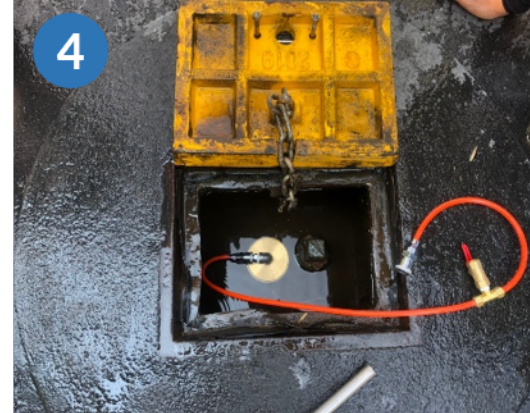
1 Check for Damage



2 Drain



3 Check water outlet



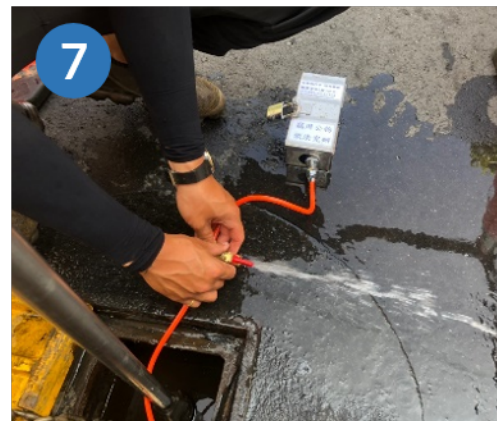
4 Installation accessories



5 Install water pressure meter



6 Locked



7 Drain



8 Installation completed

Figure 11. (A)1st Pressure measurement pattern and (B) 2nd Pressure measurement pattern.

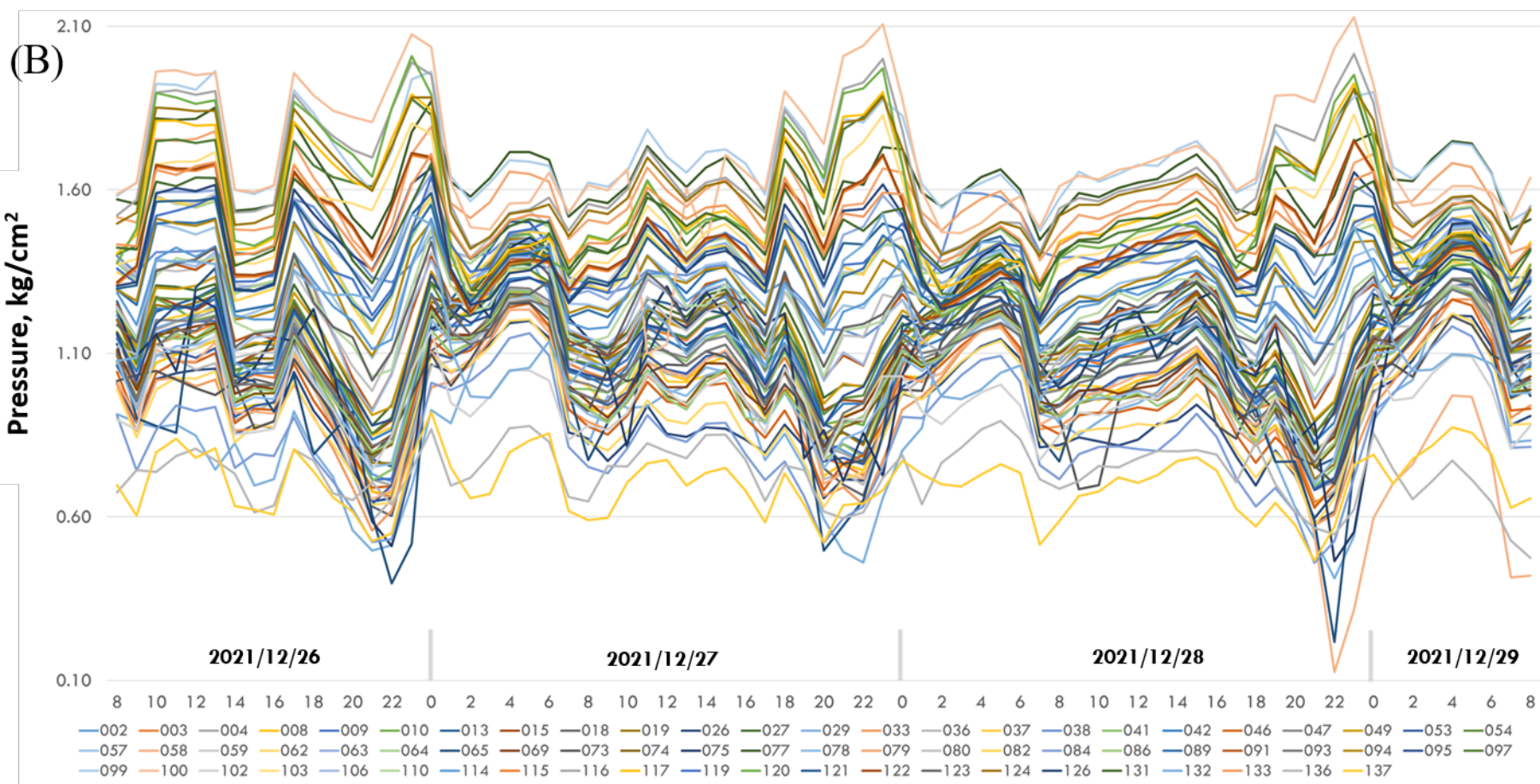
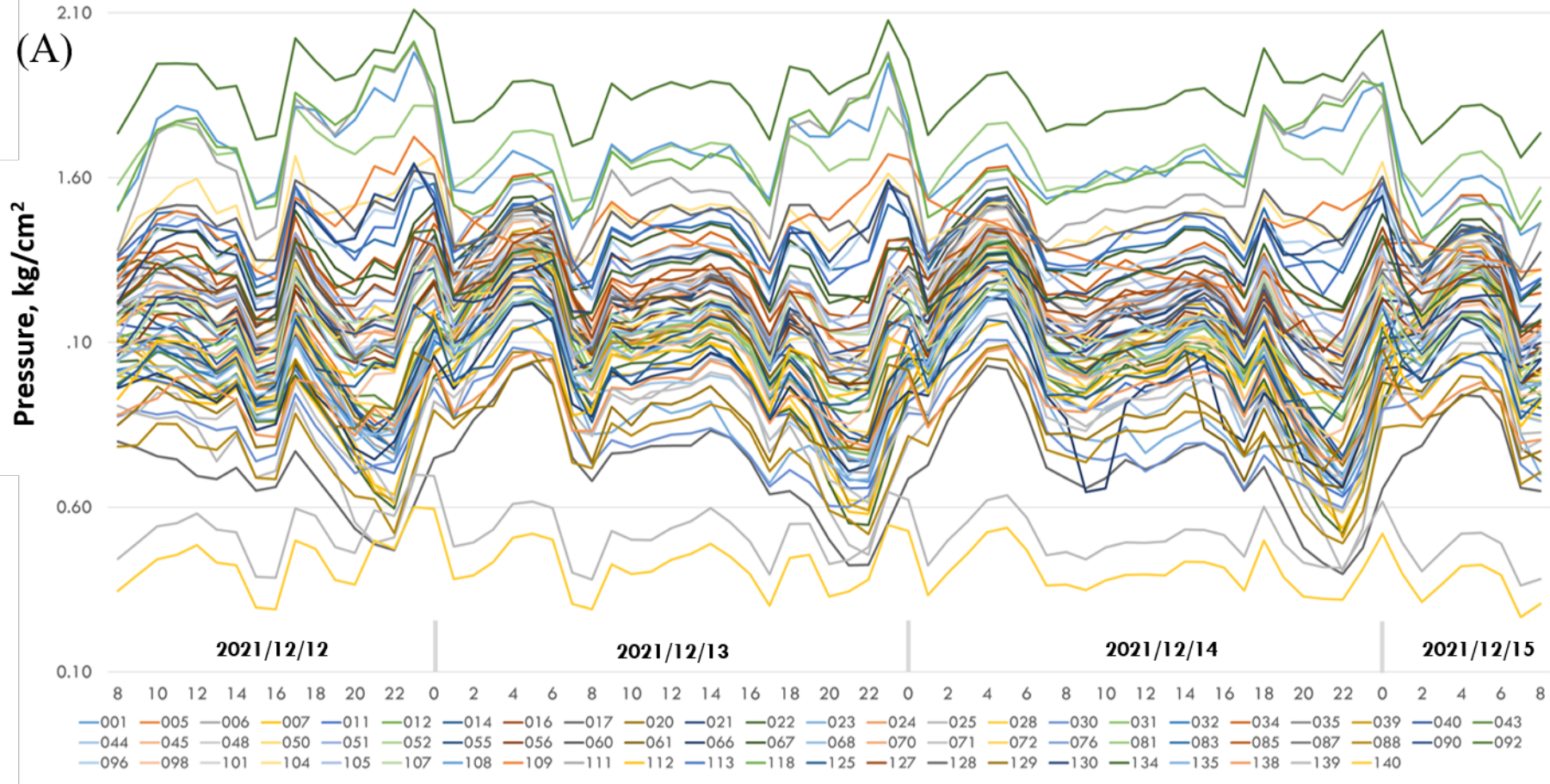


Figure 12. 2nd Obnormal point of pressure measurement.

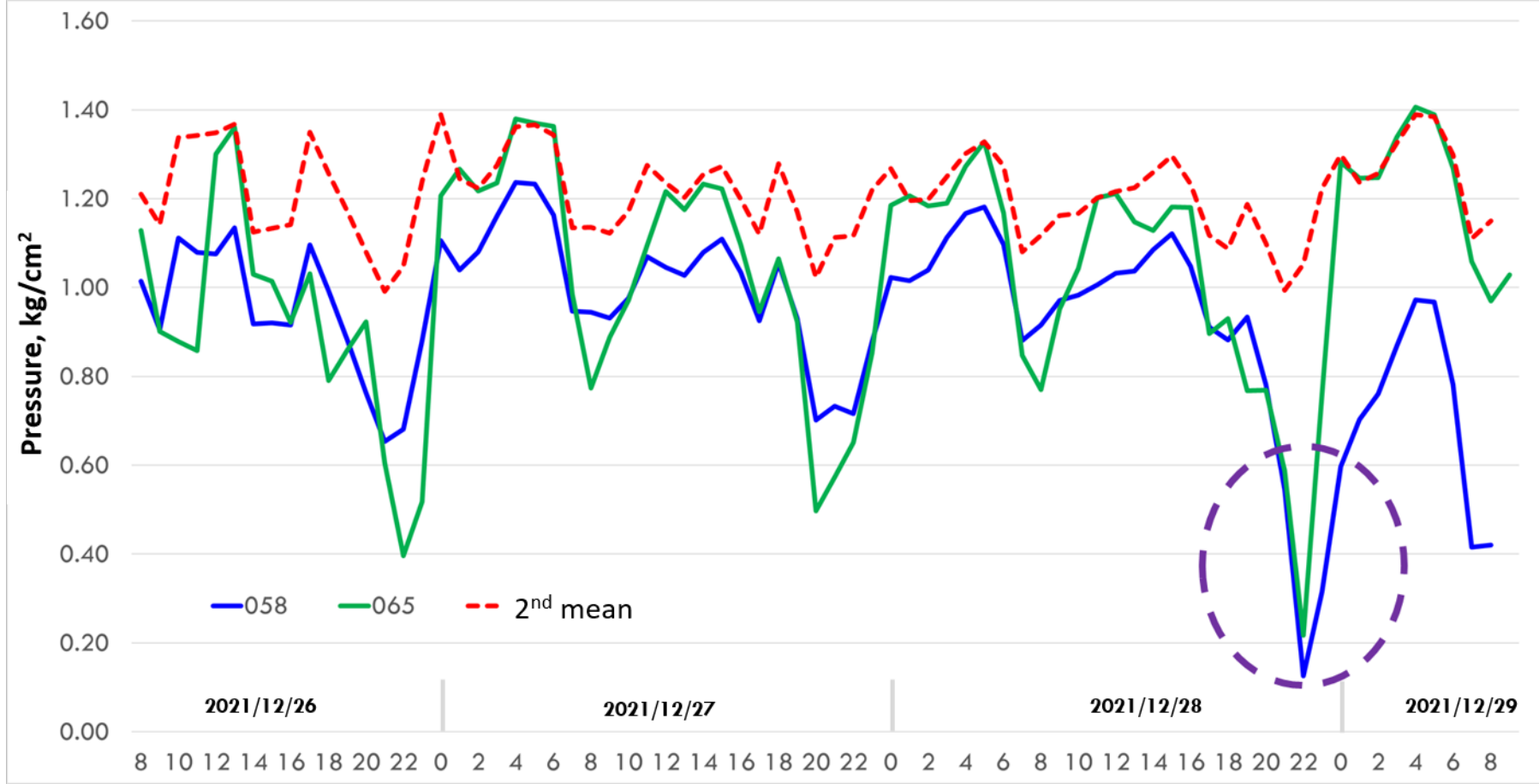
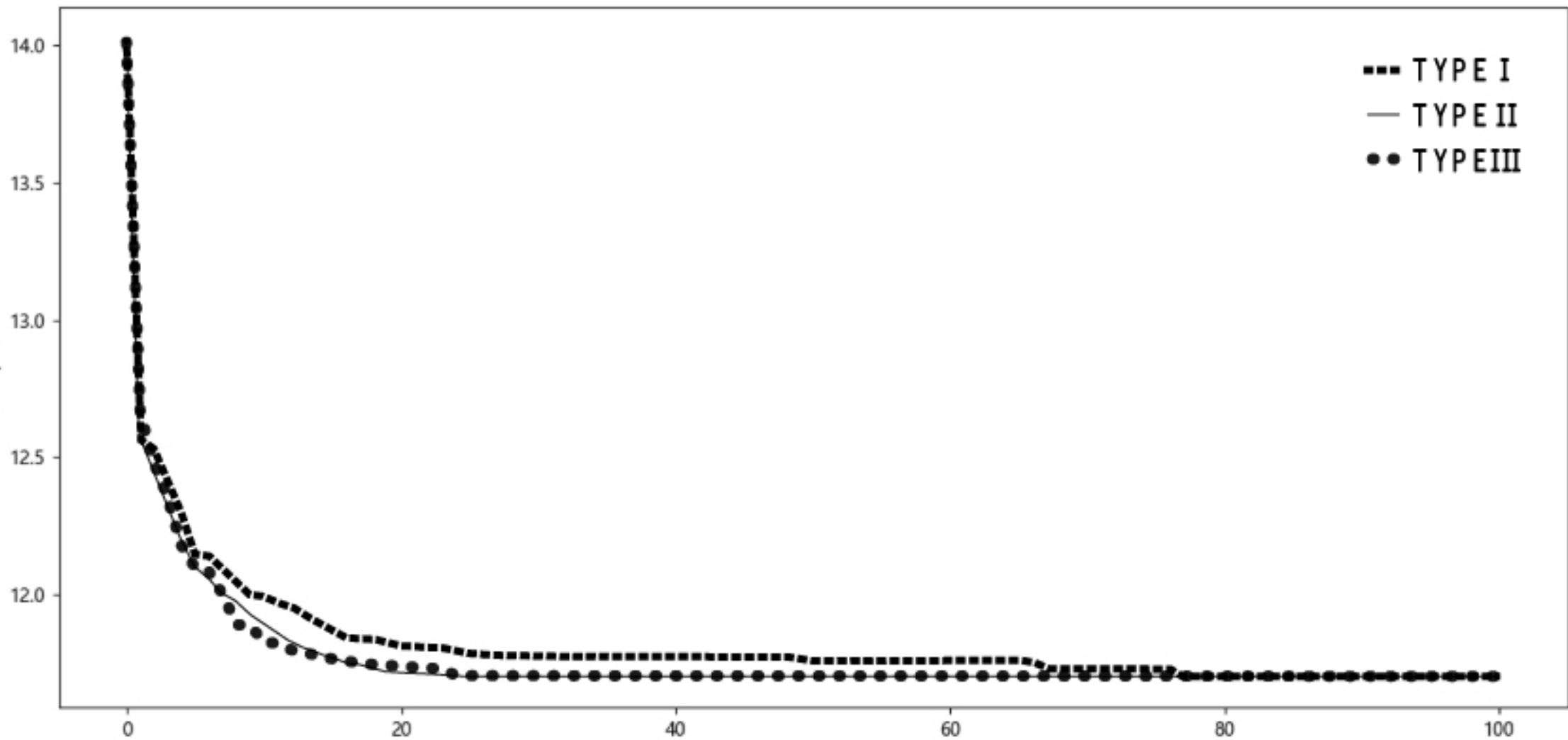


Figure 13. The Fitting Curve With Different GA Types.

delta pressure

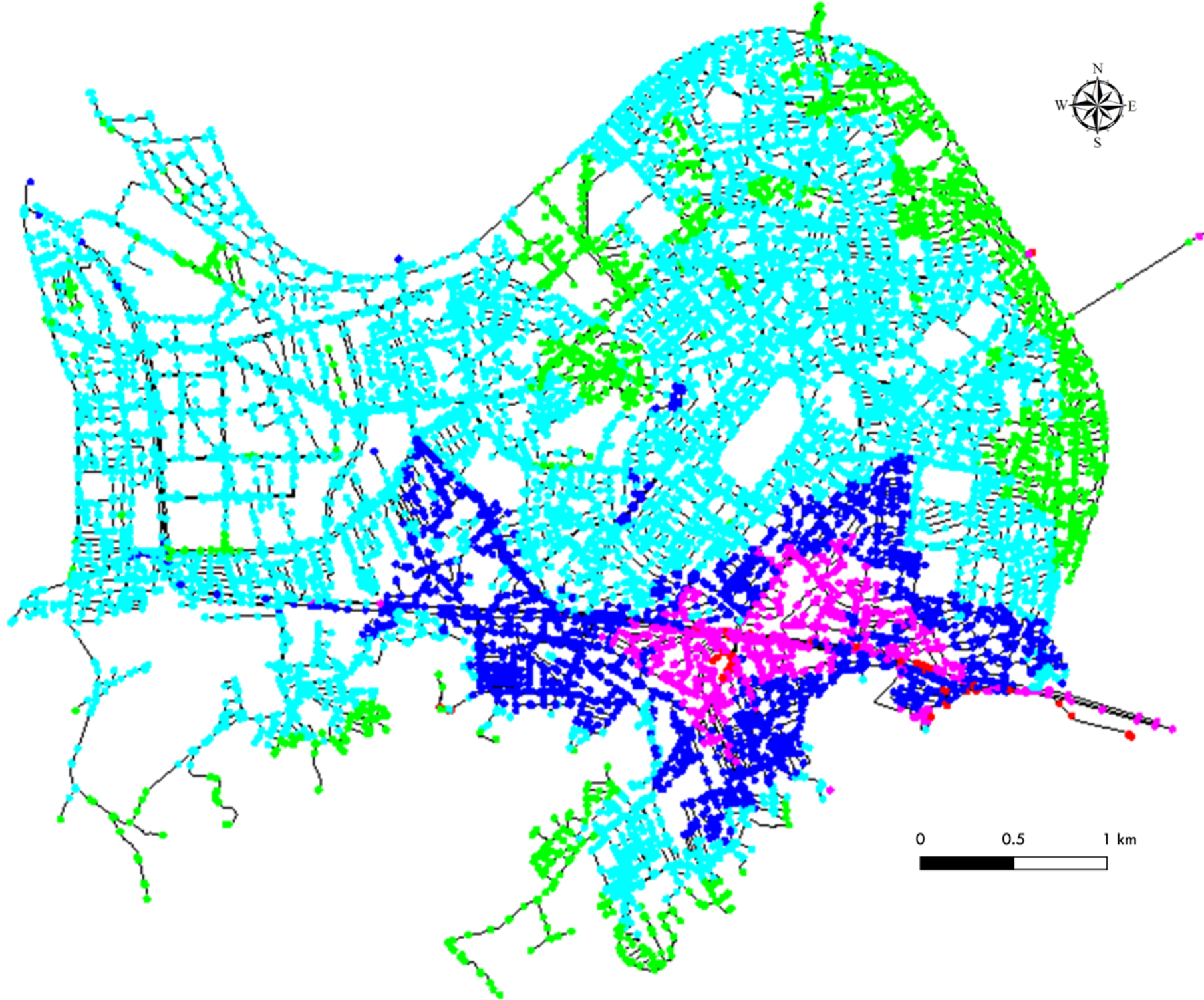


--- TYPE I

— TYPE II

••• TYPE III

Figure 14. Simulated pressure distribution map before roughness optimization.



P (kg/cm²) ● <0.5 ● 0.5~1.0 ● 1.0~1.5 ● 1.5~2.0 ● >2.0

Figure 15. Pressure difference distribution before roughness optimization.

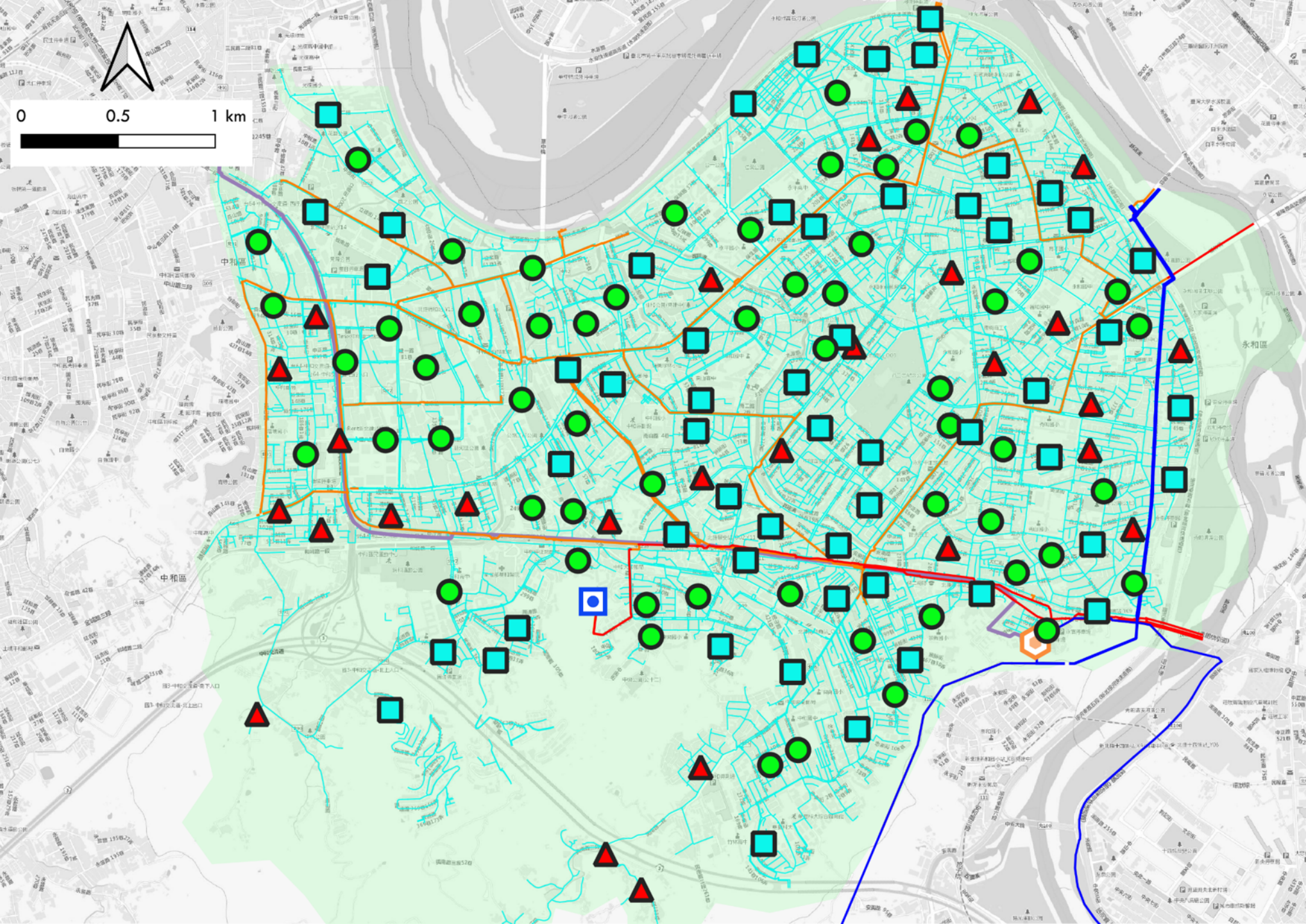


Figure 16. Pressure difference distribution after roughness optimization.

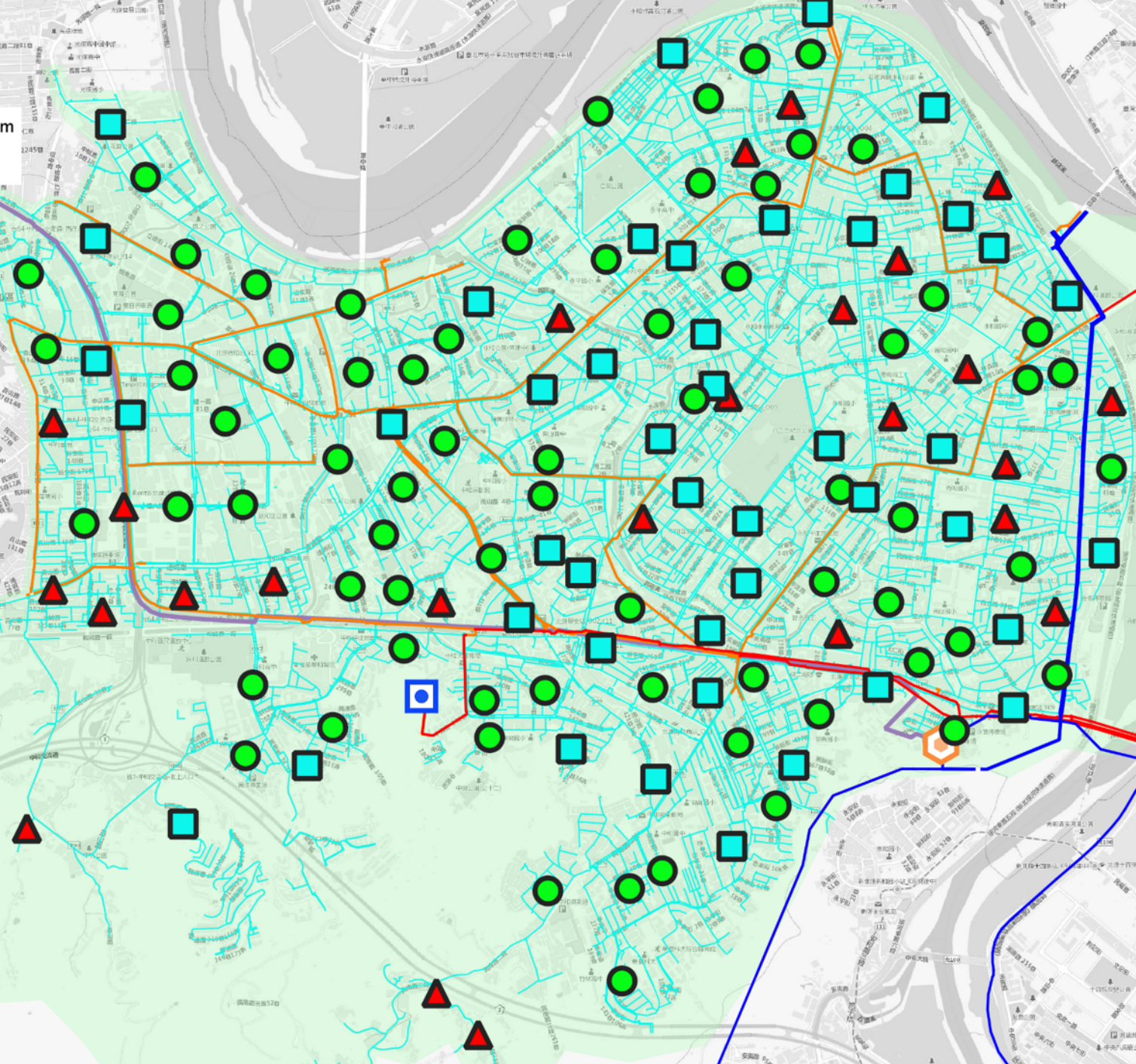
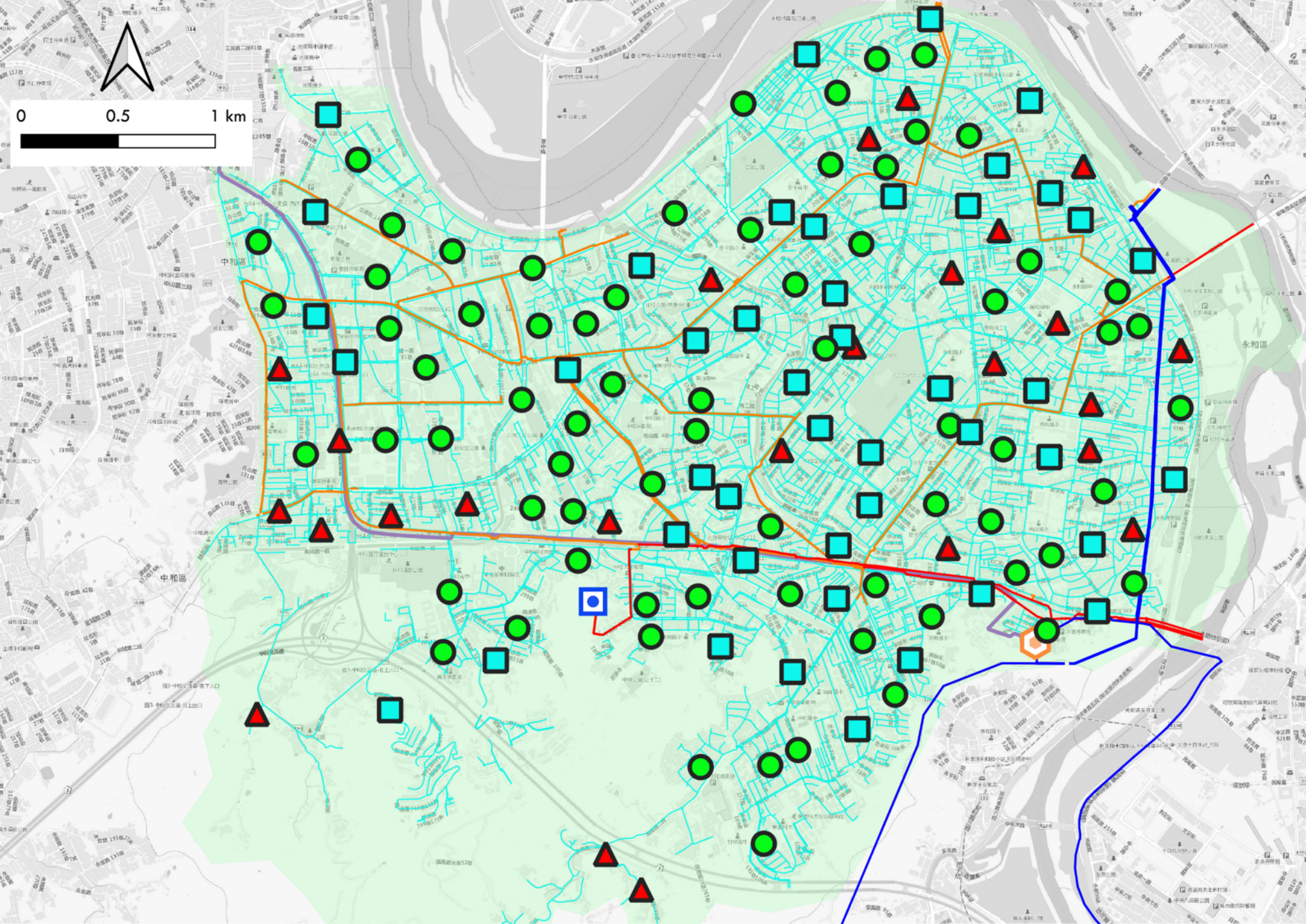
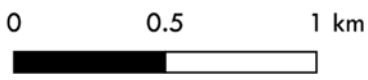
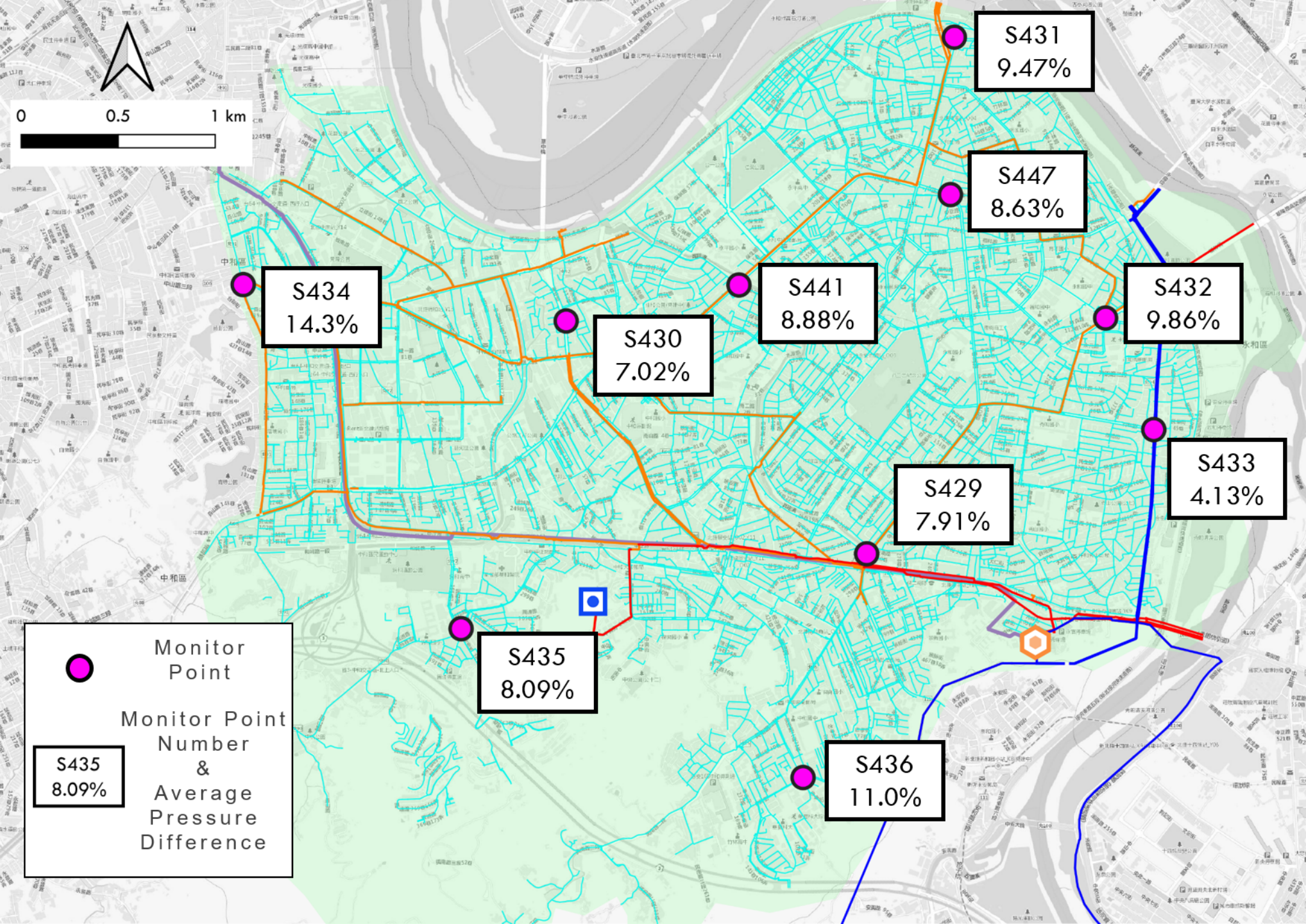


Figure 17. Specified monitoring points located at the end of the pipeline.



S434
14.3%

S430
7.02%

S441
8.88%

S447
8.63%

S432
9.86%

S431
9.47%

S429
7.91%

S433
4.13%

S435
8.09%

S436
11.0%

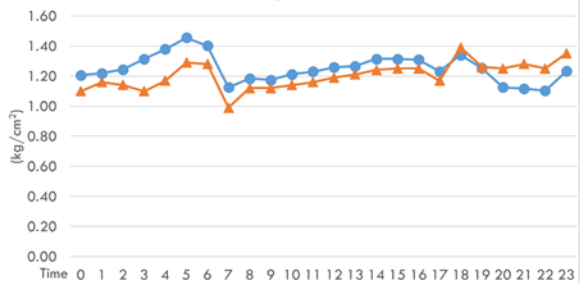
Monitor Point

Monitor Point Number & Average Pressure Difference

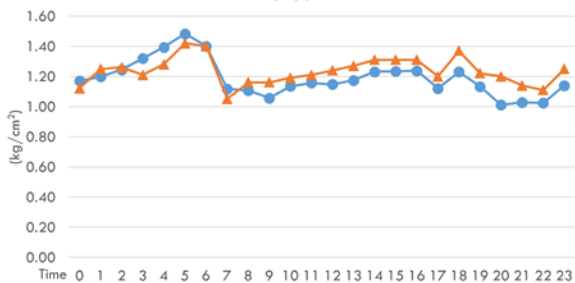
S435
8.09%

Figure 18. 24-hours pressure comparison between monitoring points and EPANET-GA simulations.

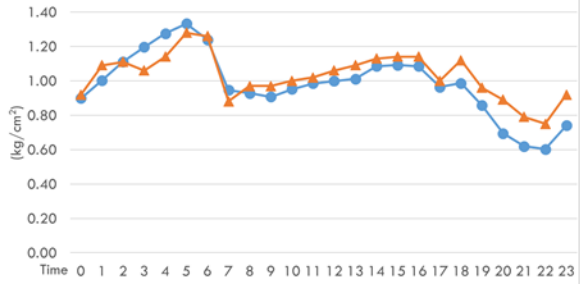
S429



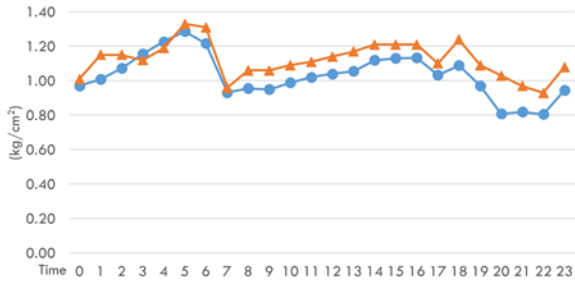
S430



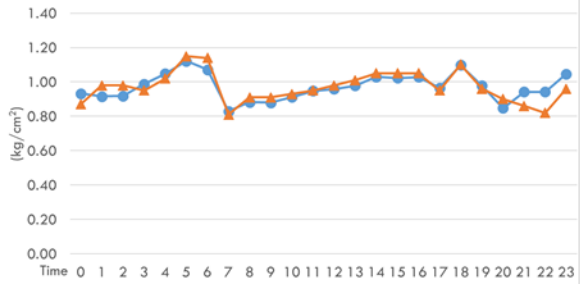
S431



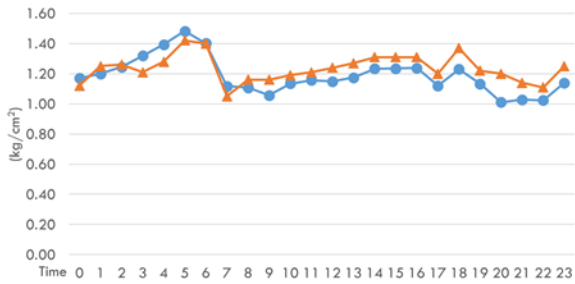
S432



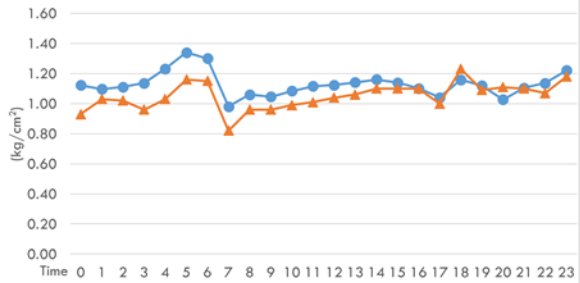
S433



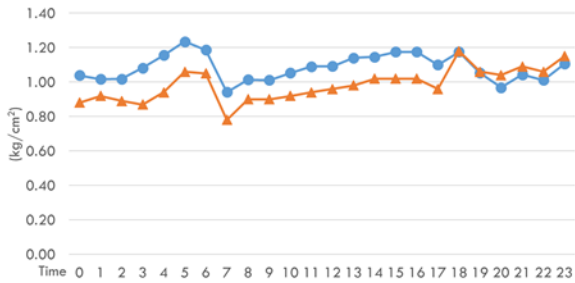
S434



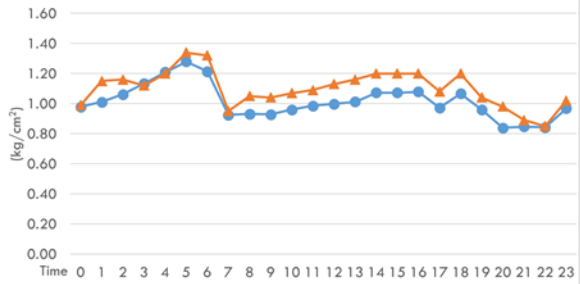
S435



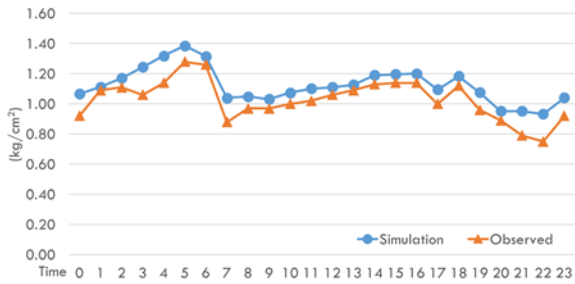
S436



S441



S447



Simulation Observed

Figure 19. Comparison bewteen WaterGEMs and EPANET-GA.

Mean Error Rate

